HYPERSPECTRAL/SPATIAL DETECTION OF EDGES (HYSPADE) ANALYSIS OF MINERAL ASSEMBLAGES AND LINEAR FEATURES AT CUPRITE, NEVADA U.S.A.

Cary M. Cox, Graduate Student
Department of Earth Systems and GeoInformation Sciences
George Mason University
Fairfax, VA 22030
ccox6@gmu.edu

ABSTRACT

The HySPADE algorithm (for hyperspectral/spatial detection of edges) is evaluated and executed against linear manmade and natural features as well as against a variety of naturally formed mineral assemblages of varying purity. The HySPADE algorithm attempts to identify the boundary between materials by generating an output cube by applying the spectral angle mapper (SAM) algorithm for each pixel in the original cube to each and every other pixel in the original cube. The output cube has as many bands as there are pixels in the original cube, with each band corresponding to the SA between its parent pixel and another original pixel as a function of spatial distribution. The final output plane is a reflection of the highest measured SA at every pixel combined into a single plane. As HySPADE has been tested thus far only against discreet manmade features imaged at high spatial resolution, this report seeks to stress HySPADE with respect to severe target complexity and weak spatial resolution. HySPADE outputs are compared to Sobel and Roberts outputs for a point of reference. HySPADE is executed against each target set over a range of user-defined thresholds in an attempt to bound the range of utility for discreet mineral deposits, mixed mineral assemblages, and manmade and natural linear features. HySPADE was found to perform consistently well against discreet mineral deposits across a broad range of thresholds. Its performance against the much more stressful target presented by the mixed mineral assemblages was comparatively reliable given the complexity of the target and the weak performance of Roberts and Sobel against the same scene. HySPADE was able to extract consistent edge information from manmade linear features over a narrow range of user-defined thresholds, but was unable to identify most naturally formed linear features. Additional target sets for HySPADE are suggested.

Key words: hyperspectral, spatial, spectral, edge detection, HySPADE

INTRODUCTION

Edge detection algorithms permeate the remote sensing community and represent one of the most effective processing techniques for analyzing features in an imagery scene. A host of algorithms have been developed to identify feature edges in all flavors of imagery, including synthetic aperture radar (SAR) imagery, panchromatic (PAN) imagery, multispectral (MSI) imagery, and most recently, hyperspectral (HSI) imagery [1], [2], [3] and [4]. A common feature of the vast majority of these algorithms is that they use either the spatial characteristics of the scene or the spectral/pixel intensity values in a scene to identify where one feature ends and another begins. Few methods attempt to leverage both the spatial and spectral aspects in a scene, leaving much of the valuable and possibly discriminating scene information unexploited.

To date, only a handful of edge detection algorithms have specifically been developed for HSI imagery. When compared to the large volume of edge detection tools developed and implemented in the PAN, MSI and SAR communities, the available HSI edge detection toolbox is populated mostly by modifications of existing MSI edge detection techniques and a few broadly applicable edge detection methods such as the Canny, Roberts and Sobel operators. While these techniques often can extract adequate edge information from HSI scenes, the unique properties of HSI cubes and the fact that the borrowed algorithms were not specifically designed for HSI imagery suggests that HSI-specific edge detection algorithms could significantly advance the reliability of edge detection operations as applied to hyperspectral cubes.

The HSI community has created two HSI-specific edge detection algorithms that take advantage of both the spectral and spatial information in an HSI scene, a significant advance ahead of the existing edge detection techniques developed by the PAN, MSI and SAR communities [5] and [6]. Published in 2007, Van der Werff et al.'s rotation-variant template matching (RTM) algorithm prosecutes a 3x1 kernel across an HSI scene by rotating the kernel at each pixel in an attempt to find the best match between the neighboring pixels' spectra and the end-member spectra at positions one and three on the RTM kernel [6]. Good spectral matches tend to mean that no edge is present at that pixel, while a poor fit indicates a possible boundary between different materials. While this method is highly dependent on the endmember spectra chosen for the rotating kernel (which implies a need for substantial a priori scene knowledge), its consideration of both the spatial and spectral qualities of a scene makes it a member of a small class of HSI algorithms that leverage both fundamental characteristics.

That small class is populated by another method: the Hyperspectral/Spatial Detection of Edges (HySPADE) algorithm, the subject of this letter. The HySPADE algorithm attempts to identify the boundary between materials by generating an output cube by applying the spectral angle mapper (SAM) algorithm for each pixel in the original cube to each and every other pixel in the original cube [5]. The output cube has as many bands as there are pixels in the original cube, with each band corresponding to the SA between its parent pixel and another original pixel as a function of spatial distribution. The final output plane is a reflection of the highest measured SA at every pixel combined into a single plane, meaning that band selection is not necessary in HySPADE because the best edge pixel (for each pixel in the original cube as detected by SAM) is automatically included in the output plane. The analyst then can simply observe (and possible histogram stretch) the final output plane and look for edge information generated by HySPADE's spectral and spatial processing of the original scene.

As will be demonstrated in the following sections, the HySPADE method will be evaluated and executed against a set of heretofore unconsidered target sets: 1) a scene populated by relatively discreet formations of naturally formed mineral deposits, 2) a scene dominated by a variety of mixed mineral assemblages, and 3) a scene containing long, linear manmade and natural features. To date, HySPADE has been tested only against synthetic data and relatively high spatial resolution HSI scenes containing discreet manmade structures. While HySPADE performed well against the manmade targets on high resolution imagery, it has yet to be tested against natural targets, stressing or otherwise. This report seeks to fill that gap by advancing the understanding of HySPADE functionality against natural features in a complex scene.

OBJECTIVES

This study has a primary and secondary objective. Most importantly, through a series of threshold-varied tests, this study seeks to evaluate the effectiveness of the HySPADE algorithm as applied to mineral assemblages and linear features. During the pursuit of the primary objective, four new contributions will be realized. First, to date, HySPADE has been executed only against discreet man-made structures and simulated data. The mineral assemblage targets examined herein will determine HySPADE's effectiveness against broad, natural targets in an actual scene. Secondly, HySPADE will be executed against a 10,000-pixel cube; previous work was performed on a much smaller 2500-pixel cube. Thirdly, HySPADE will be executed against 188-band AVIRIS data (after bad-band removal), while previous work was performed on 166-band HYDICE data. Finally, HySPADE will be executed against relatively low spatial resolution AVIRIS imagery (~17m), while previous work was done against high resolution HYDICE data (1-2m). In sum, HySPADE will be performed against a much larger data set containing significantly more challenging targets imaged at a lower resolution. AVIRIS's advantage in spectral resolution is nominal.

The study's secondary objective concerns HySPADE's performance against the AVIRIS data as compared to the performance of the Roberts and Sobel Operators. This objective is not intended to produce a rigorous performance comparison among Roberts, Sobel and HySPADE – to do so would require an exhaustive accounting of the thousands of variations in kernel size, threshold and histogram stretches available for each algorithm. Instead, the inclusion of the Roberts and Sobel operators simply is intended to provide a general reference point for estimating the performance of HySPADE against broad, natural targets.

METHODOLOGY

Data Acquisition and Pre-Processing

An AVIRIS image of Cuprite, Nevada was obtained from Dr. Ronald Resmini from George Mason University. The image was delivered in standard 224-band, 400-2500nm VNIR/SWIR format having already been converted to reflectance. The complete image is 614 samples X 511 lines and covers an area rich in a variety of minerals, topographies and manmade structures. The image also had been processed for bad bands, and a double-check of bad bands indicated that no other bands needed to be removed. Ultimately, bands 107-118 and 152-175 were removed (H_2O absorption), leaving a 188-band cube to be used for the study. The spatial resolution is roughly 17m throughout the scene.

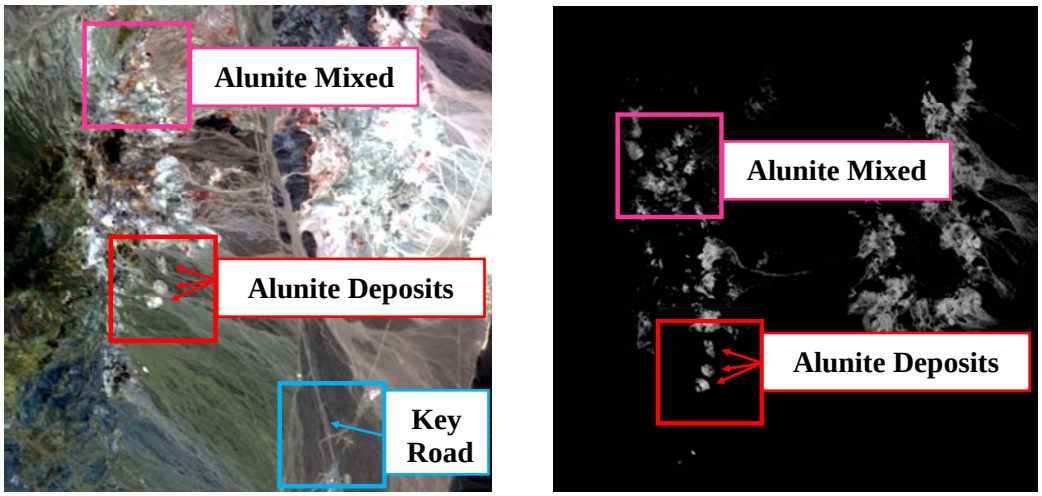

Figure 1. On the left are three subscenes selected from the overall Cuprite scene. Each scene is 100x100 and 188 bands. The area in the red box is the Alunite Dominant subscene, the area in the pink box is the Alunite Mixed subscene, and the area in the blue box is the Road Network subscene. On the right, the in-scene SAM output clearly extracts the three relatively discreet Alunite deposits in the Alunite Dominant subscene outlined in red. The Alunite Mixed subscene outlined in pink was chosen for the broad distribution of Alunite throughout the area.

Subscene Selection

Three 100x100 subscenes were selected from the overall Cuprite scene. Two subscenes were selected in order to test HySPADE's performance against mineral assemblages, and a single scene was chosen to measure HySPADE's reliability against long, linear targets. The left image in Figure 1 portrays the overall Cuprite scene and the three subscenes.

To test HySPADE's performance against mineral targets, one subscene was selected for its well-known discreet deposits of the mineral Alunite, and the second was chosen for its broad mix of Alunite and other minerals [7]. The subscene with the relatively pure Alunite deposits is referred to as the "Alunite Dominant" subscene, while the second subscene is referred to as the "Alunite Mixed" subscene. Specifically, the Alunite scenes were selected by executing an in-scene Spectral Angle Mapper (SAM) operation against the entire scene, stretching the output to optimal display, and visually choosing the two areas. The Alunite Dominant subscene was chosen for the crisp border between the Alunite and surrounding materials as well as for the relative purity of the deposits themselves. The Alunite Mixed subscene was selected because of the broad mixture of Alunite with other minerals – a reality clearly indicated by the SAM output on the right-hand side of Figure 1.

For comparison, SAM was executed using the library spectrum "Alunite3.spc." Since the output did not render the discreet Alunite deposits as well as the in-scene SAM output and severely washed out the Alunite in the Alunite Mixed subscene, the library spectrum SAM output was not utilized for subscene selection.

The Road Network subscene was selected by visually examining the three-color composite image of the Cuprite scene. The confluence of several different road types and widths makes the area an attractive test target for

examining HySPADE's effectiveness against long linear targets. A large building is visible towards the southern end of the subscene, and a mineral deposit to the northeast also is of interest. The boundary between the hills and flatlands to the west is examined, as well. The key target, however, is the long road running the length of the scene from north-northwest to south-southeast.

HySPADE Code Acquisition, Modification and Execution

The HySPADE code was acquired in its native C programming language format directly from Resmini. He provided the finished code in a format that allowed modifications to be made in any C-code compiler. All modifications and compiling were accomplished with Microsoft C++ 2008 Express Edition® software.

In this study, HySPADE was modified to operate against the AVRIS dataset, which required three changes to the source code. First, the code was configured to process the 188-channel cube instead of the original 166-channel HYDICE cube. Secondly, the code was modified to accept a 100-line by 100-sample cube. These settings were kept for the duration.

The third and most important modification to the HySPADE source code was the alteration of the "edge" threshold – a modification that was systematically executed throughout the study. Essentially, HySPADE determines the existence of an edge pixel according to a simple first-order comparison of a multiple of the standard deviation of the set of values generated for each SA-spectrum [1]. The "multiple" is a user-defined threshold generally fixed between 0.25σ and 5.00σ, and is the fundamental determinant of whether HySPADE will indicate an edge for a given pixel in a given scene.

Specifically, thresholds from 0.25σ and 5.25σ were applied to each test cube in order to sufficiently capture the range of effectiveness for the HySPADE algorithm against each. Output planes that generated no edge information tended to cluster at the highest threshold values and were omitted from this letter. Selective stretching was necessary for most output cubes in order to maximize output consistency among the tests – given the enormous volume of possible outputs derivable from stretching and the subtle changes apparent from stretch to stretch, introducing systematic stretching to the study would have expanded its scope unreasonably.

Roberts and Sobel Execution

The Roberts and Sobel Operators are available in the ENVI® suite of tools, which was used for all such executions in this study. While, ENVI® provides only non-editable versions of the operators (each with a default 3x3 kernel), this limitation did not significantly affect the study given that Sobel and Roberts outputs were simply used as guide posts. Ultimately, Roberts and Sobel were applied to each of the test cubes and their outputs compared to the HySPADE output planes from the same cubes.

Along with the generation of a three-color composite, selective stretching was performed for selective bands in the Roberts and Sobel output cubes. While band selection and stretching of these outputs introduces an element of uncontrolled selectivity, the effect on the study is minimal due to the role these operators are playing – HySPADE is the algorithm of study, not Roberts and Sobel.

RESULTS

Alunite Dominant Subscene

Figure 2 shows the Roberts and Sobel operators applied to the 100x100 Alunite Dominant subscene. In each case, a three-color composite is provided to indicate each operator's performance against all targets in the subscene. Alongside is provided a single band selected for its rendering of the Alunite deposits in the center of the scene.

The Roberts output faithfully represents much of the edge information surrounding the Alunite deposits as well as much of the edge information among the assemblages to the west. Its performance against the northernmost Alunite deposit was not as reliable, as indicated by the fuzzy boundaries on the east and west side of the assemblage. The output also indicates several "false" boundaries along many of the terrain contours in the scene. While these boundaries certainly are true spatial boundaries, they are not mineral boundaries – an anomaly that reinforces the necessity of understanding feature characteristics within a scene.

The Sobel output also reliably depicts most of the edge information surrounding the three central Alunite deposits. Edge information also is visible among the assemblages to the west. Edges are slightly broader in the Sobel output and crisp edges are slightly more discernable. The "false" edges along the terrain contours are slightly brighter, as well.

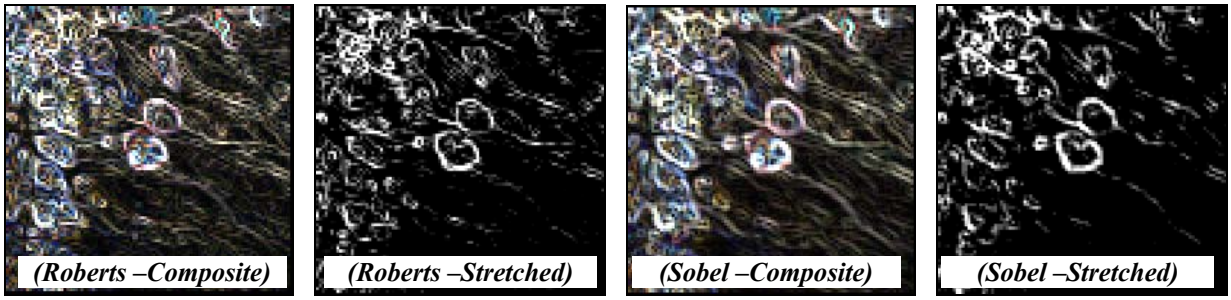

Figure 2. On the left, the Roberts operator is applied to the Alunite Dominant Subscene. The Roberts operator clearly depicts the boundaries between the Alunite deposits and the surrounding mineral assemblages. Band 100 was histogram stretched in order to optimize edge information around the Alunite deposits. Edge information also is visible among the assemblages to the west. On the right, the Sobel operator applied to the Alunite Dominant Subscene. Much like the Roberts output, the Sobel operator clearly depicts the boundaries between the Alunite deposits and the surrounding mineral assemblages. Band 100 was histogram stretched in order to optimize edge information around the Alunite deposits. Edge information also is visible among the assemblages to the west, and the overall quality of edge information in the scene is much smoother than the Roberts output.

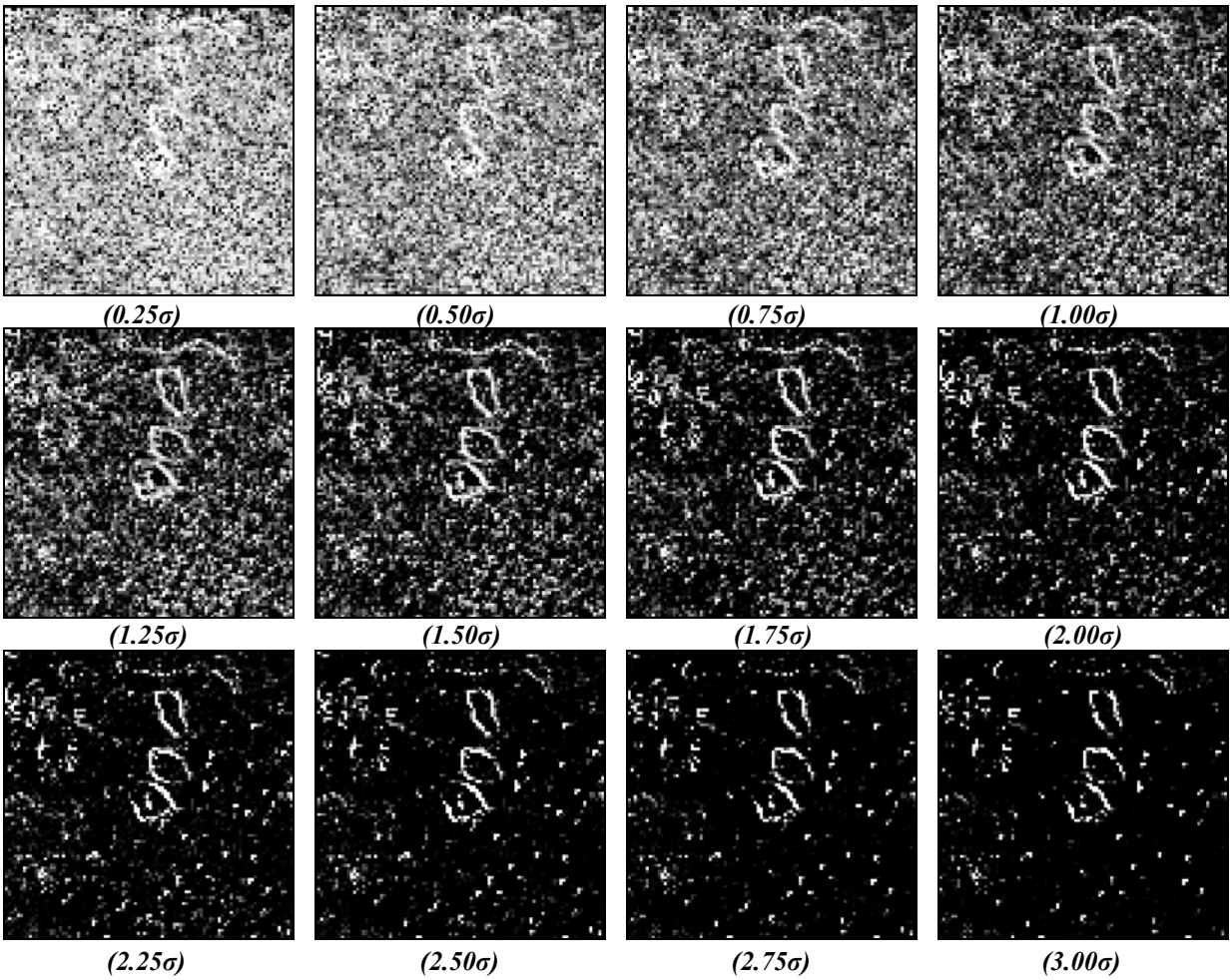

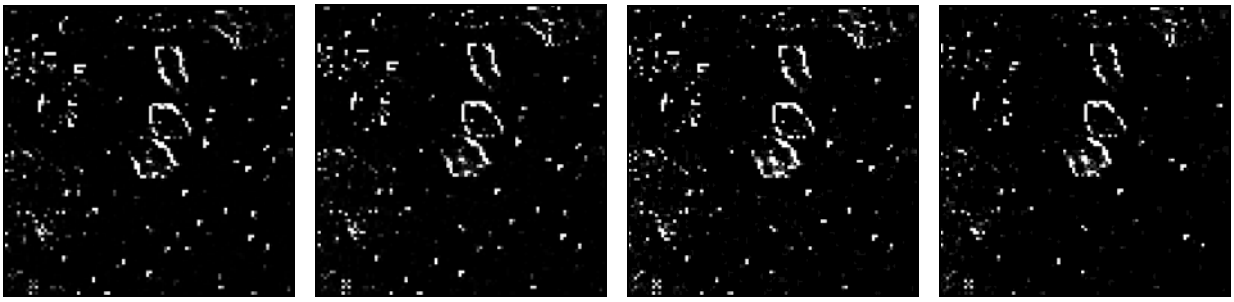

(3.25σ) *(3.50σ)* *(3.75σ)* *(4.00σ)*

Figure 3. HySPADE applied to the Alunite Dominant subscene. Thresholds are indicted below each output plane, and no histogram stretching was applied. HySPADE reliably depicts edge information around the Alunite deposits. Even at very low thresholds, some edge information can be extracted without histogram stretching. At higher thresholds, the edge information around the alunite deposits is resilient, although coherent edge information among the assemblages to the west is not discernable at any threshold.

Figure 3 presents the HySPADE algorithm applied to the Alunite Dominant subscene. Thresholds between 0.25σ and 4.00σ were chosen, and edge information is visible at all thresholds. Edge information can be extracted from even the lowest thresholds without histogram stretching, and edge information is still visible at the highest thresholds. HySPADE performed well against the northernmost Alunite deposit, as well. The "sweet spot" for HySPADE against the Alunite Dominant target appears to be roughly between 2.00σ and 3.25σ.

Alunite Mixed Subscene

Figure 4 shows the Roberts and Sobel operators applied to the 100x100 Alunite Mixed subscene. In each case, a three-color composite is provided to indicate each operator's performance against all targets in the subscene. Alongside is provided a single band selected for its overall rendering of the Alunite assemblages in the scene.

The Roberts output performed poorly against the mineral assemblages in the subscene. Edge information is largely incoherent throughout the scene with the exception of the land/water boundary in the southern portion of the subscene. Some scattered coherent edge information is identifiable along the eastern portion of the area, and some edge information is decipherable along the large Alunite deposits to the northwest. These deposits, however, are behaving more like discreet deposits rather than mixed assemblages and Robert's performance along these edges cannot be interpreted as the operator's capability against a mixed assemblage target.

The Sobel output appears superior to the Roberts output but still produced mixed results against the mineral assemblages in the scene. The broader edges in the Sobel output offer modest improvement against the assemblages in the eastern portion of the scene, and the edges of several small deposits can be identified. Significant improvement can be achieved through histogram stretching, as seen in Figure 4. The land/water boundary is clearly recognizable, as well.

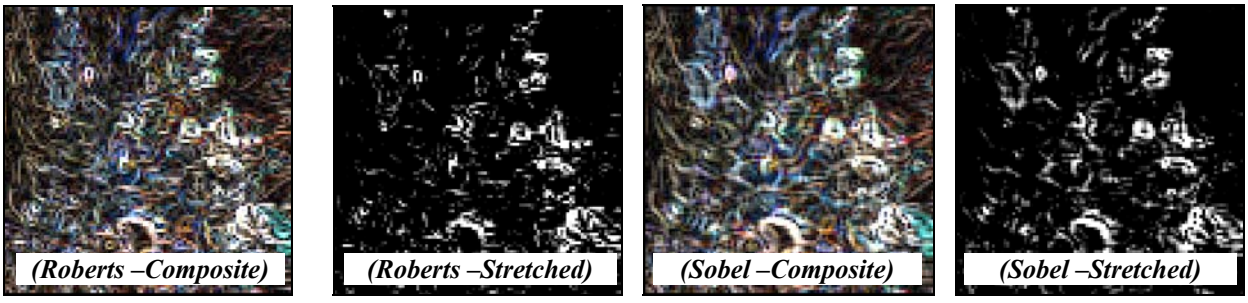

Figure 4. On the left, the Roberts operator is applied to the Alunite Mixed Subscene. The Roberts operator fails to clearly depict the boundaries between the Alunite assemblages and the surrounding mineral assemblages. Band 18 was histogram stretched in order to optimize edge information around the Alunite assemblages, but did not significantly improve the interpretability of the image. Some edge information

also is visible among the assemblages to the east, and the land/water boundary in the southern portion of the image is accurately rendered. On the right, the Sobel operator is applied to the Alunite Mixed Subscene. The Sobel operator outperformed the Roberts operator in the scene, but still generated mixed results against the boundaries between the Alunite assemblages and the surrounding mineral assemblages. Band 15 was histogram stretched in order to optimize edge information around the assemblages, which modestly improved the interpretability of the image. The land/water boundary in the southern portion of the image is accurately rendered, as well.

Figure 5 presents the HySPADE algorithm applied to the Alunite Mixed subscene. Thresholds between 0.25σ and 4.00σ were chosen, and the interpretability of edge information varies by thresholds. In general, as the HySPADE threshold increased, so did the clarity of edge information. Unlike the Alunite Dominant subscene, coherent edge information is largely confined to the middle threshold values between roughly 1.25σ and 2.25σ. Edge information is nearly completely lost at the lowest and highest thresholds.

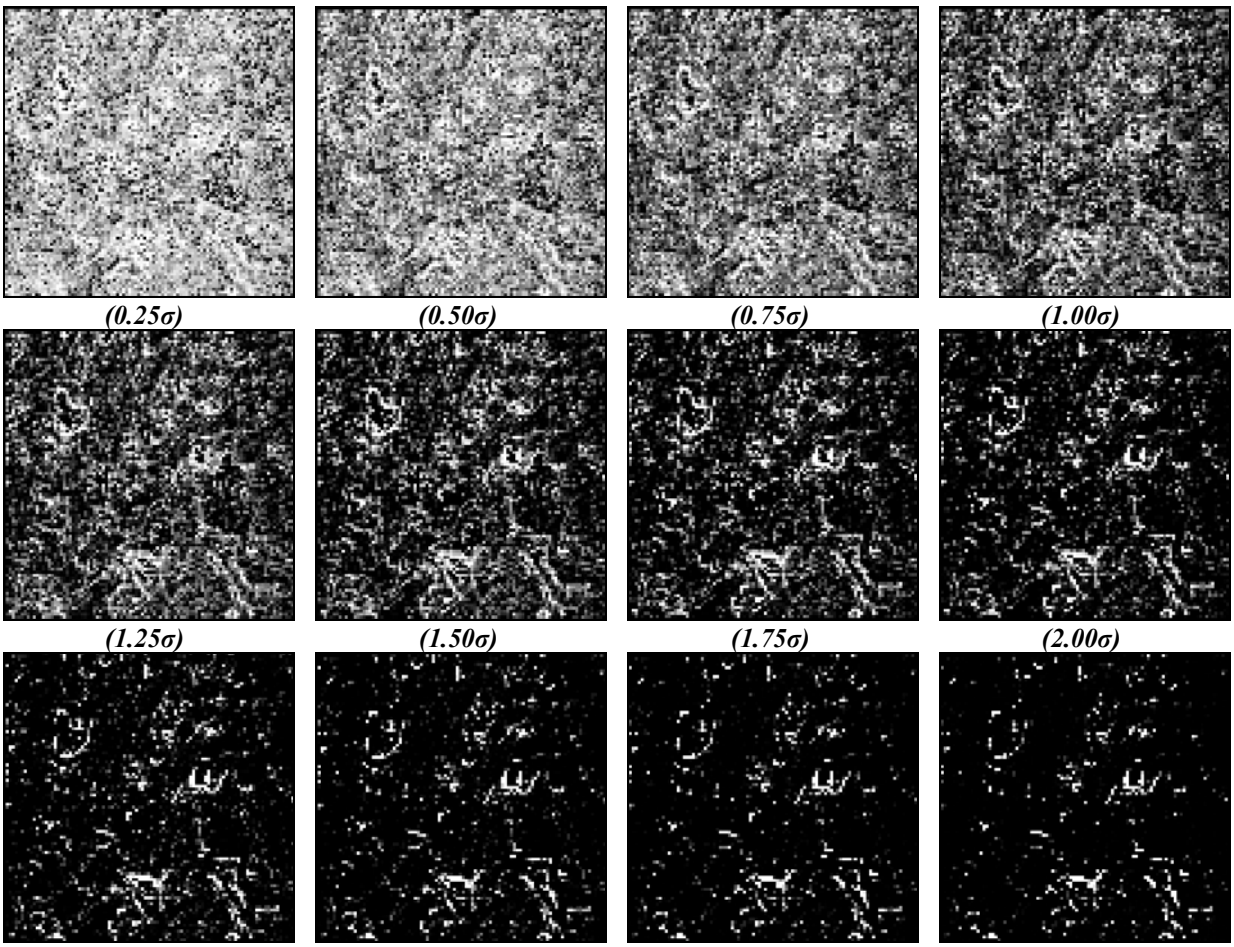

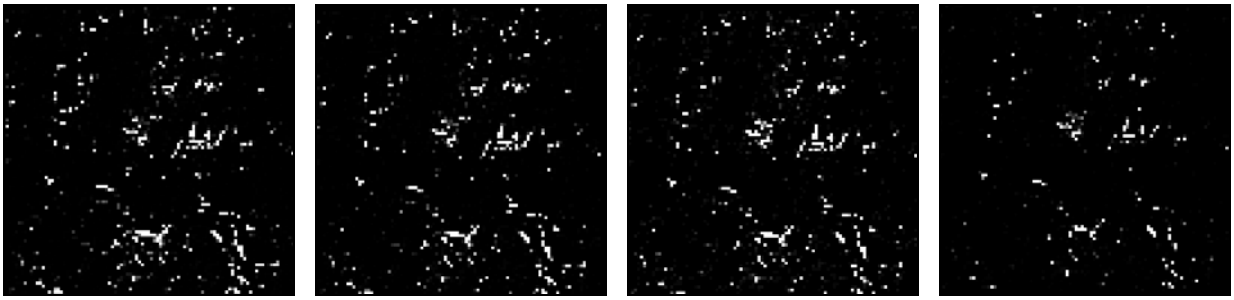

(3.25σ) *(3.50σ)* *(3.75σ)* *(4.00σ)*

Figure 5. HySPADE applied to the Alunite Mixed subscene. Thresholds are indicted below each output plane, and no histogram stretching was applied. HySPADE depicts edge information around the Alunite assemblages to varying degrees of accuracy, but performs remarkably well given the complexity of the target. Edge information is largely lost at lower and higher thresholds, leaving the middle thresholds as the most reliable indicators of edge information.

Road Network Subscene

Figure 6 shows the Roberts and Sobel operators applied to the 100x100 Road Network subscene, respectively. In each case, a three-color composite is provided to indicate each operator's performance against all targets in the subscene. Alongside is provided a single band selected for its overall rendering of the linear features in the scene.

The Roberts output performed well against both the manmade and natural linear features in the subscene. Edge information is reliable for all of the roads in the scene. The interpretability of the contours along the hills to the west are highly dependent on band selection and histogram stretching, but are largely recognizable even in the color composite. In general, band stretching of the Roberts output was more helpful against linear targets compared to mineral assemblages. However, band stretching can suppress subtle terrain features such as the contours in the drainage network in the hills to the west.

The Sobel output showed some improvement over the Roberts output. The main linear feature is reliably rendered in nearly all bands of the Sobel output and is clearly distinguishable from its surroundings. Again, the boundaries of the mineral deposit to the northeast are clearly recognizable and the cluster of roads to the south is more clearly defined. Like Roberts, histogram stretching improves the output.

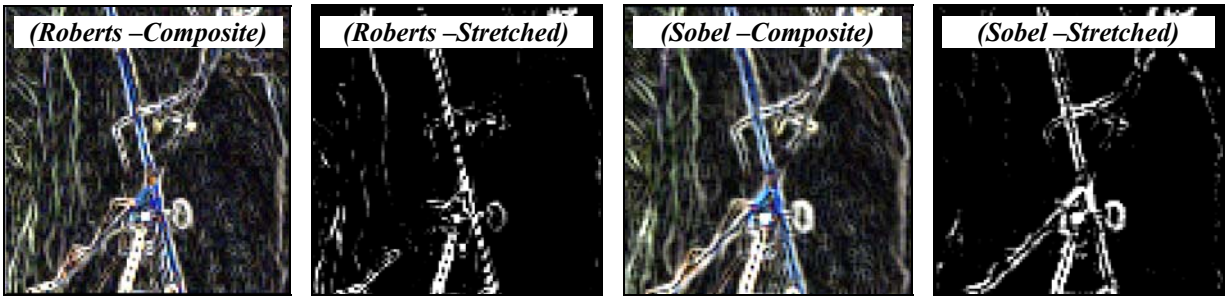

Figure 6. On the left, the Roberts operator is applied to the Road Network Subscene. The Roberts operator clearly depicts the linear features in the scene. Band 140 was histogram stretched in order to optimize edge information along the main linear feature, and modestly improved the interpretability of the feature. Reliable edge information also is visible along several of the smaller roads in the scene as well as along the contours to the west. The mineral deposit to the northeast is clearly recognizable. On the right, the Sobel operator is applied to the Road Network Subscene. The Sobel operator outperformed the Roberts operator, and generated reliable results against the linear features. Band 5 was histogram stretched in order to optimize edge information along the primary manmade linear feature in the scene, which modestly improved interpretability.

Figure 7 presents the HySPADE algorithm applied to the Road Network subscene. Thresholds between 0.25σ and 5.00σ were chosen for publication due to the resiliency of edge information for the major linear feature in the

scene even at very high thresholds. Oddly, the main road in the scene is not adequately resolved until 3.25σ, when it appears rather abruptly in both the unstretched and stretched scenes. A possible explanation for the absence of edge information pertaining to the main linear target at low thresholds and its sudden appearance at a relatively high threshold could be the low volume of pixels populated by the width of the road. Alternatively, the roadside material could be very similar to the road material, allowing the road to effectively "hide" inside the signature of its immediate environment by defeating HySPADE's SAM subroutine. Overall, HySPADE fully resolved the main linear feature beyond 3.25σ.

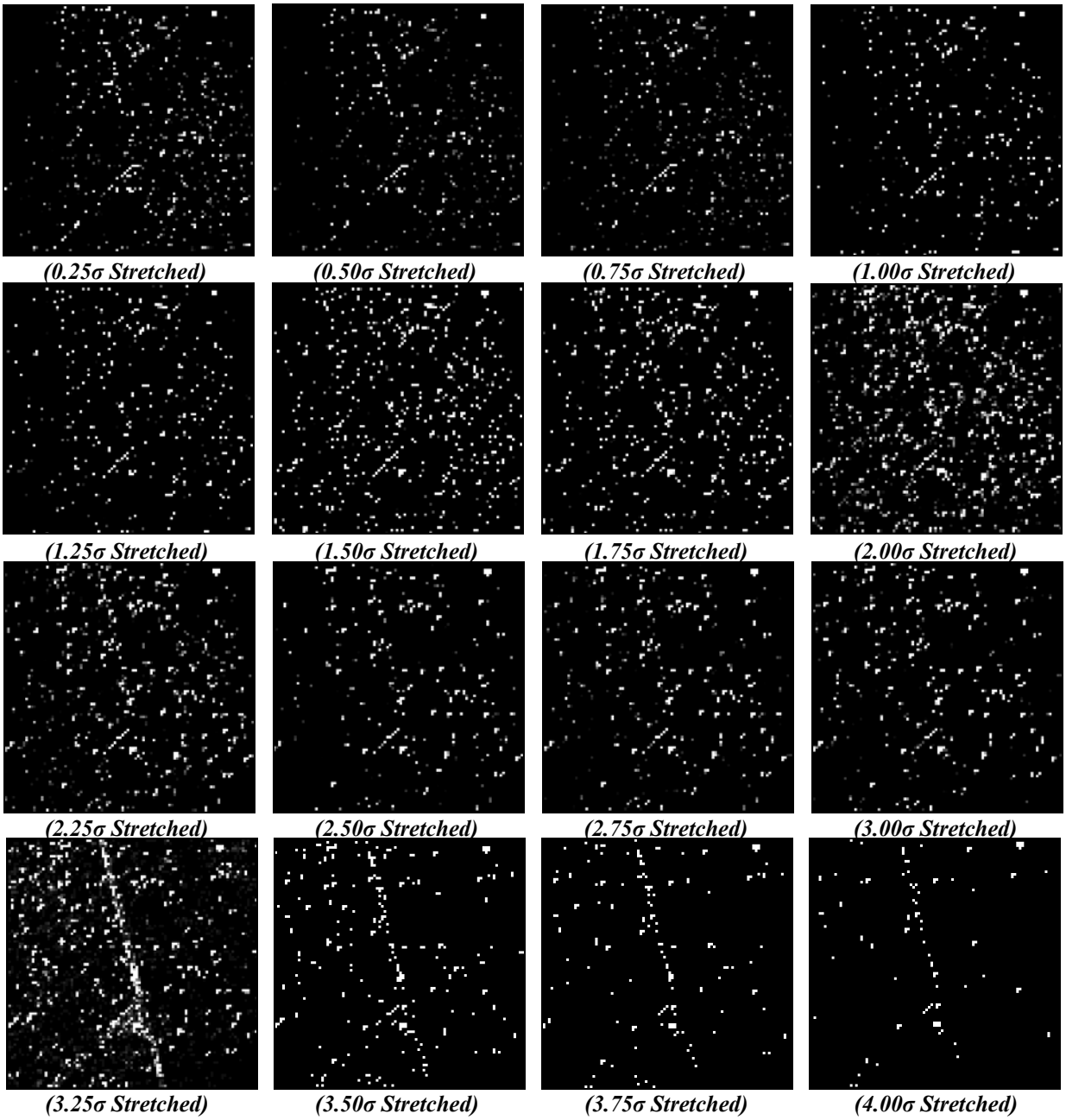

(0.25σ Stretched) *(0.50σ Stretched)* *(0.75σ Stretched)* *(1.00σ Stretched)*

(1.25σ Stretched) *(1.50σ Stretched)* *(1.75σ Stretched)* *(2.00σ Stretched)*

(2.25σ Stretched) *(2.50σ Stretched)* *(2.75σ Stretched)* *(3.00σ Stretched)*

(3.25σ Stretched) *(3.50σ Stretched)* *(3.75σ Stretched)* *(4.00σ Stretched)*

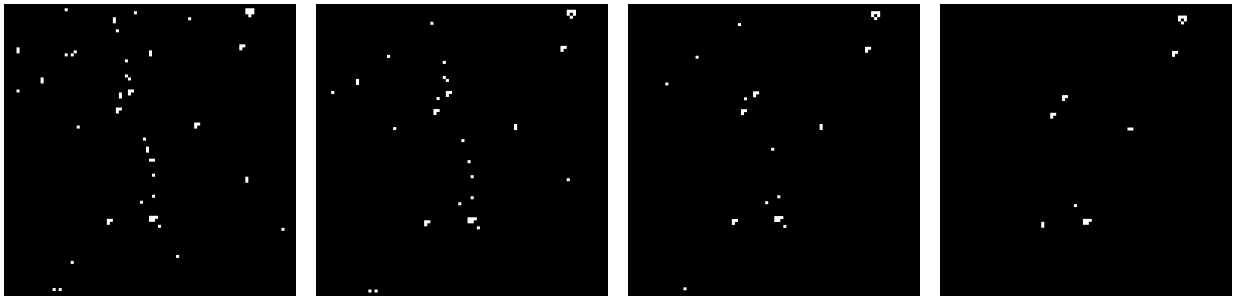

(4.25σ Stretched) *(4.50σ Stretched)* *(4.75σ Stretched)* *(5.00σ Stretched)*

Figure 7. HySPADE applied to the Road Network subscene: 0.25σ – 1.00σ. Thresholds are indicted below each output plane, and histogram stretching has been applied to each scene because much of the edge information contained in the low to middle threshold outputs is wholly indecipherable without stretching.

The smaller roads in the scene are quickly filtered out by thresholds beyond 1.00σ, a comparatively low threshold. Even then, significant histogram stretching is required to coax the edge information out of the output planes. HySPADE failed to resolve the linear features along the western portion of the scene at all thresholds. Edge information along the primary northeast to southwest running road is visible in the histogram stretching of the lowest executed thresholds (<0.25σ). Oddly, with the exception of a segment to the north, the coherency of the feature is not sustained as thresholds increase above 0.25σ, but does reappear again at higher thresholds beginning at 1.25σ. Coherency continues to improve between 2.25σ and 3.00σ, and is largely filtered out by 3.75σ.

DISCUSSION

HySPADE Performance against Alunite Dominant Subscene

As seen throughout Figures 3, 5 and 7, HySPADE can reliably extract edge information against a variety of manmade and natural targets. Its performance against the Alunite Dominant scene was sufficient to clearly identify the edges of the three dominant Alunite deposits, and outperformed both Sobel and Roberts in clarifying the boundaries of the northernmost Alunite deposit. The Alunite deposits begin to take shape at approximately 1.00σ and were fully resolved by about 2.50σ - 2.75σ. Edge information was still discernable until roughly 4.25σ – 4.50σ, but declined rapidly by 5.00σ.

A key finding of this study is that mineral assemblages appear to require higher thresholds sufficient to extract reliable edge information compared to the lower thresholds' ability to identify manmade structures. This finding is justified by Resmini's HySPADE outputs that target multiple manmade features, which were clearly resolved on HYDICE imagery processed at 0.25σ [1]. While Resmini's results were obtained from higher spatial resolution imagery, the possibility that the limited spatial resolution AVIRIS imagery is grossly distorting the relationship between thresholds and manmade and naturals features is remote. Additionally, as seen in the Road Network output planes in Figure 7, manmade features in AVIRIS imagery can be resolved at 0.25σ and 0.50σ. Consequently, discreet mineral deposits appear to require higher thresholds to fully resolve their outlines.

HySPADE Performance against Alunite Mixed Subscene

As seen throughout Figure 5, several HySPADE output planes performed remarkably well against the stressing target presented by a scene populated with multiple overlapping and intermixed mineral assemblages. Taken as a whole, the results were mixed; neither the lowest nor highest thresholds were able to generate interpretable results. Mid-range threshold outputs, however, generated coherent edges scattered throughout the image – a clear reflection of the mixed assemblages in the scene. Several small but discreet assemblages were extracted by HySPADE along the eastern portion of the scene, and the land/water boundary to the south is well depicted across the range of thresholds. The linear feature in the southeast portion of the scene is clearly recognizable in a number of output planes, as well.

In general, the "sweet spot" for mixed mineral assemblages appears to be between roughly 1.25σ and 2.25σ – a range that is indicative of the need to retain a volume of edge information sufficient to resolve indistinct boundaries but reduced enough so as not to overwhelm the mixed assemblage boundaries with false positives.

Also, the range of utility for the Alunite Mixed subscene is substantially lower than the optimal range for the Alunite Dominant subscene but higher than that required to resolve discreet manmade targets. Again, this is a function of the need to filter out much of the noise in the scene while leaving sufficient edge information to identify blurry boundaries between mixed assemblages. Clearly, a delicate balance of thresholds and histogram stretching is required when examining a target dominated by mixed mineral assemblages. This balance will almost certainly vary among different scenes at different resolutions.

Overall, given the modesty of the Roberts and Sobel outputs, the coherent edges identified by HySPADE in the eastern portion of the scene suggest that HySPADE performs comparatively well against mixed mineral assemblages. The target was purposefully chosen to stress the HySPADE algorithm, which was not expected to generate a set of crisp white boundaries between intimately mixed targets. Indeed, such an output would have been inconsistent with the mixed nature of the scene as indicated by the SAM output. More than likely, the combination of the spectral component with the spatial consideration of the HySPADE algorithm allowed it to outperform the Roberts and Sobel operators, which consider only the spatial and pixel intensity values in a scene.

HySPADE Performance against Road Network Subscene

As seen in Figure 7, HySPADE reliably extracted edge information from the major linear features in the scene, most notably the primary road running from northwest to southeast. While the primary road did not reappear until 3.25σ, when it resolved rather abruptly, it remained resilient beyond 4.00σ and was still recognizable even into the highest thresholds executed in the study, 5.00σ-5.25σ. As mentioned above, a possible explanation for the absence of edge information pertaining to the main linear target at moderate thresholds and its sudden appearance at a relatively high threshold could be the low volume of pixels populated by the width of the road. Alternatively, the roadside material could be very similar to the road material, allowing the road to effectively "hide" inside the signature of its immediate environment by defeating HySPADE's SAM subroutine.

Significant histogram stretching was required to maximize the output quality for most thresholds, most notably at the lowest thresholds. The northeast to southwest running road in the southern portion of the scene was recognizable only at the lower thresholds, and even then only after significant stretching. A "wasteland" of sorts then stretched between roughly 1.75σ and 3.00σ, where very little edge information was observable and little overall improvement was seen. After 3.25σ, only the major road in the scene produced adequate edge information. The smaller roads and linear natural features to the west were completely filtered out at the highest thresholds.

SUMMARY

The HySPADE edge detection algorithm was executed against three 188-band, 100x100 subscenes extracted from an AVIRIS image of Cuprite, Nevada in order to test its ability to extract edge information from scenes dominated by mineral assemblages or long linear features. The Alunite Dominant scene was selected in order to test HySPADE's ability to demarcate the boundary between relatively discreet mineral deposits and their surrounding environment. HySPADE was found to be highly capable of identifying the edges of the Alunite deposits in the scene, and did so at a measurably higher threshold than is required to identify the edges of manmade objects. The second scene, Alunite Mixed, was selected in order to test the ability of HySPADE to extract edge information from a scene dominated by mixed mineral assemblages with few crisp boundaries. At lower thresholds than were required for useful edge detection in the Alunite Dominant subscene, HySPADE was able to reliably identify several assemblage edges in the scene, indicating that HySPADE is capable of competently processing stressful targets. The third and final subscene, Road Network, was selected for its network of long linear features, both natural and manmade. HySPADE was found to be capable of reliably extracting the edges of the primary road beyond 3.25σ but not below it, and capable of extracting edge information from the smaller roads at 1.00σ but not above it. HySPADE's performance against manmade linear features was superior to its performance against natural linear features.

FUTURE DIRECTIONS

HySPADE has yet to be executed against a variety of targets, both natural and manmade, simplistic and stressing: i) manmade features on the water, particularly the open ocean, ii) manmade and natural features in high-relief topographies, iii) natural and manmade features on snowy terrain, iv) natural and manmade features in a dense urban environment, v) gasses and aerosols, vi) surface mediums such as oil slicks on seawater, vii) subsurface features, both land and water, and viii) natural disaster areas.

ACKNOWLEDGEMENTS

Support for this work was ably provided by Dr. Ronald Resmini and the Department of Earth Systems and GeoInformation Sciences at George Mason University, Fairfax, VA.

REFERENCES

Richards, J.A., and Xiuping Jia, 2006. *Remote Sensing Digital Image Analysis, An Introduction, Fourth Edition*, Springer-Verlag, Berlin, 118, 439.

Schou, J., H. Skriver, A.A. Nielsen, and K. Conradsen, 2003. CFAR edge detector for polarimetric SAR images, *IEEE Transactions on Geoscience and Remote Sensing*, 41(1), 20-32.

Haijian, Ma, Qin Qiming, Du Shihong, Wang Lin, and Jin Chuan, 2007. Road extraction from ETM panchromatic image based on dual-edge following, *IEEE International Geoscience and Remote Sensing Symposium*, 460-463.

Bakker, W. and K. Schmidt, 2002. Hyperspectral edge filtering for measuring homogeneity of surface cover types, *ISPRS Journal of Photogrammetry and Remote Sensing*, 56(4), 246-256.

Resmini, R.G., 2004. Hyperspectral/Spatial Detection of Edges (HySPADE): An algorithm for spatial and spectral analysis of hyperspectral information, *Proceedings of SPIE 5425*, 443-442.

Van der Werff, H., F. Van Ruitenbeek, M. Van der Meijde, F. Van der Meer, S. De Jong, and S. Kalubandara, 2007. Rotation-variant template matching for supervised hyperspectral boundary detection, *IEEE Geoscience and Remote Sensing Letters*, 4(1), 70-74.

Resmini, R.G., M.E. Kappus, W.S. Aldrich, J.C. M.E. Harsanyi, and Anderson, 1997. Mineral mapping with Hyperspectral Digital Imagery Collection Experiment (HYDICE) sensor data at Cuprite, Nevada, U.S.A., *International Journal of Remote Sensing*, 18(7), 1553-1570.